Condensed Exponential Correlation Functions in Multicomponent Polymer Blends Measured by X-ray Photon Correlation Spectroscopy

Megan L. Ruegg,[†] Amish J. Patel,[†] Suresh Narayanan,[‡] Alec R. Sandy,[‡] Simon G. J. Mochrie,[§] Hiroshi Watanabe,[⊥] and Nitash P. Balsara*[,†,#]

Department of Chemical Engineering, University of California, Berkeley, California 94720; Argonne National Laboratory, Argonne, Illinois 60439; Department of Physics, Yale University, New Haven, Connecticut 06520; Institute for Chemical Research, Kyoto University, Uji, Kyoto 611-0011, Japan; and Materials Sciences Division and Environmental Energy Technologies Division, Lawrence Berkeley National Laboratory, University of California, Berkeley, California 94720

Received May 26, 2006; Revised Manuscript Received August 7, 2006

ABSTRACT: X-ray photon correlation spectroscopy experiments were conducted on bicontinuous microemulsion and lamellar phases in polystyrene/polyisoprene/poly(styrene-*b*-isoprene) blends. Regardless of the microstructure, the scattering intensity autocorrelation function at low temperatures in the vicinity of the primary X-ray scattering peak, $g_2(q,t)$ (q is the scattering vector), was found to be a condensed exponential, i.e., $g_2(q,t) \sim \exp\{-[t/\tau(q)]^{\alpha}\}$ with $\alpha > 1$. This is in direct contrast to previous observations of exponential and stretched exponential correlation functions ($\alpha \leq 1$) in microstructured materials comprising polymers as well as small molecules. At higher temperatures, more conventional stretched exponential correlation functions are recovered. We suggest that condensed exponential relaxation functions may be related to the spontaneous breakup of microsctructure.

Introduction

There is considerable interest in the characterization of thermally driven motion of self-assembled fluids such as micelles, colloidal suspensions, lamellae, microemulsions, etc. Much of our understanding of this motion is based on light photon correlation spectroscopy (LPCS), i.e., dynamic light scattering. This technique enables the measurement of the scattering vector (q) dependent dynamic structure factor, $S(q,t)$. In the case of incompressible two-component systems, $S(q,t)$ is the spatial Fourier transform of the density−density autocorrelation function $\langle \rho_A(\mathbf{r}',t)\rho_A(\mathbf{r},0)\rangle$, where $\rho_A(\mathbf{r},t)$ is the concentration of one of the components (A) at position $\mathbf{r}$ and time t. The key feature that distinguishes LPCS from techniques such as dielectric relaxation and rheology is the ability to observe relaxation on a range of specific length scales depending on the accessible range of q. In LPCS, the accessible length scales of observation ($\sim 1/q$) are centered about 500 nm. This range is large in comparison to the characteristic size of typical self-assembled structures, which, for polymeric systems is about 10 nm. The development of X-ray photon correlation spectroscopy (XPCS)[1−3] and quasi-elastic neutron scattering (QENS) enable measurement of the dynamic structure factor on 10 nm length scales.

Photon correlation spectroscopy (LPCS or XPCS) experiments can be used to determine the scattering intensity correlation function, $g_2(q,t)$, which is closely related to $S(q,t)$. These measurements enable the determination of $G(1/\tau)$, the distribution of relaxation processes due to thermal motion

$$g_2(q,t) \equiv \frac{\langle I(q,0)\, I(q,t)\rangle}{\langle I(q,t)\rangle^2} = 1 + \beta\left(\int_0^{\infty} G(1/\tau_r)\mathrm{e}^{-t/\tau_r}\, \mathrm{d}(1/\tau_r)\right)^2 \quad (1)$$

where τ_r is a variable of integration. In the simplest case, a single relaxation process dominates, i.e., $G(1/\tau_r)$ is a delta function $\delta(1/\tau_r - 1/\tau)$, and $g_2(q,t)$ is given by a single-exponential function:

$$g_2(q,t) = 1 + \beta \mathrm{e}^{-2t/\tau(q)} \quad (2)$$

and τ is the characteristic relaxation time for relaxation of structure at length scales $\sim 1/q$. In many cases, however, the relaxation of structure occurs via multiple processes. If they are widely separated in time scales, then $G(1/\tau)$ takes on a multipeaked form. There are, however, many examples wherein the relaxation processes are not widely spaced in time. A prominent example of such a case is $g_2(q,t)$ of dense colloidal suspensions.[4] In this case, the decay of $g_2(q,t)$ at small length and time scales is rapid due to the local motion of the colloids, but the decay slows down at longer length and time scales due to the caging of colloids by their neighbors. It is believed that the solidlike properties of all glasses arise from such effects.[5,6] In such cases, it is often convenient to approximate $g_2(q,t)$ by a stretched exponential:

$$g_2(q,t) = 1 + \beta \exp(-2[t/\tau(q)]^{\alpha}) \quad (3)$$

where the stretching parameter α, which must be less than or equal to unity, is a measure of width of the relaxation spectrum. Stretched exponential functions are found in a wide variety of systems. For example, Zilman and Granek have studied the dynamics of membrane-containing phases theoretically[7,8] and have obtained stretched exponential correlation functions with $\alpha = 2/3$ for aligned membranes. For unaligned membranes, α values slightly greater than 2/3 are obtained (the absolute value depends on the bending modulus and temperature). This behavior has been observed experimentally in a variety of systems, such as block copolymer vesicles[3] and oil/water/surfactant microemulsions and lamellae.[9−12]

In this paper we describe XPCS data obtained from lamellar and microemulsion phases obtained by mixing two incompatible homopolymers A and B and an A−B diblock copolymer. We

[†] Department of Chemical Engineering, UC Berkeley.
[‡] Argonne National Laboratory.
[§] Yale University.
[⊥] Kyoto University.
[#] Lawrence Berkeley National Laboratory, UC Berkeley.

10.1021/ma061183y CCC: $33.50
Published on Web 11/09/2006

Table 1. Characterization of Polymers[a]

polymer	M_w (kg/mol)	PDI
PS	2.9	1.02
PI	2.5	1.05
PS−PI	6.6−6.9	1.02

[a] M_w is the weight-averaged molecular weight; PDI $= M_w/M_n$ where M_n is the number-average molecular weight.

Table 2. Blend Compositions

blend	ϕ_{PS}	ϕ_{PI}	ϕ_{PS-PI}
B11.5	0.443	0.443	0.115
B20	0.400	0.400	0.200

demonstrate that over a wide range of conditions the measured $g_2(q,t)$ is consistent with eq 3. However, the values of α obtained are significantly greater than unity. The correlation functions of these systems thus decay more rapidly than a single exponential. This result is outside the scope of the standard XPCS and LPCS framework which is based on eq 1. Since $G(\tau)$ can be no sharper than a single delta function, $g_2(q,t)$ obtained from this framework cannot decay any faster than exponentially. We are not aware of any framework that is consistent with our observations.

Our experimental system comprises a symmetric A−B diblock copolymer added to a critical mixture of immiscible A and B homopolymers. The static thermodynamic properties of these mixtures has been well documented both experimentally and theoretically.[13−43] A variety of phases are observed, including microstructured phases such as lamellae and bicontinuous microemulsions. The dynamics of microstructured polymeric systems, both in solution and in the melt, has been previously probed by LPCS.[17,44−54] Other authors have studied the stress relaxation in A/B/A−B polymer microemulsions using rheology[55−57] and the self-diffusion of diblock copolymer chains in the melt or in solution with pulsed field gradient nuclear magnetic resonance (NMR).[58−63] All of the previous data are entirely consistent with eq 1.[17,44−63]

Experimental Methods

Our experimental system consists of poly(styrene-*b*-isoprene) (PS−PI) added to a critical mixture of polystyrene (PS) and polyisoprene (PI). The system was designed on the basis of extensive characterization of A/B/A−B systems by Bates, Lodge, and co-workers.[13−17] PI and PS−PI were synthesized via anionic polymerization in benzene at room temperature. All reagents were purified under high vacuum. For the diblock copolymer, an aliquot of the first block was isolated and terminated for characterization purposes, prior to the addition of the second block. The polymers were dried fully under vacuum until they reached constant weight. PS was purchased from Polymer Source.

The molecular weight distributions of the polymers were determined on a Waters 2690 gel permeation chromotography system with a Viscotek triple detector. The three detectors (light scattering, viscometry, and refractometry) enabled the determination of the absolute number- and weight-averaged molecular weights ($\overline{M_n}$ and $\overline{M_w}$) and the polydispersity index (PDI) of the homopolymers and the block copolymer precursor. Nuclear magnetic resonance spectroscopy was used to determine the block ratio in the diblock copolymer. The characteristics of the polymers used in this study are summarized in Table 1.

Multicomponent PS/PI/PS−PI blends were created by dissolving the components in benzene and freeze-drying the homogeneous mixture under vacuum. When a sample was prepared from the freeze-dried blend for a specific experimental measurement, it was ultimately annealed at $T = 110$ °C, which would ensure complete removal of the solvent. The characteristics of the multicomponent blends utilized in this study are shown in Table 2. We focus on two blends: B20 with 20 vol % diblock copolymer and B11.5 with 11.5 vol % diblock copolymer.

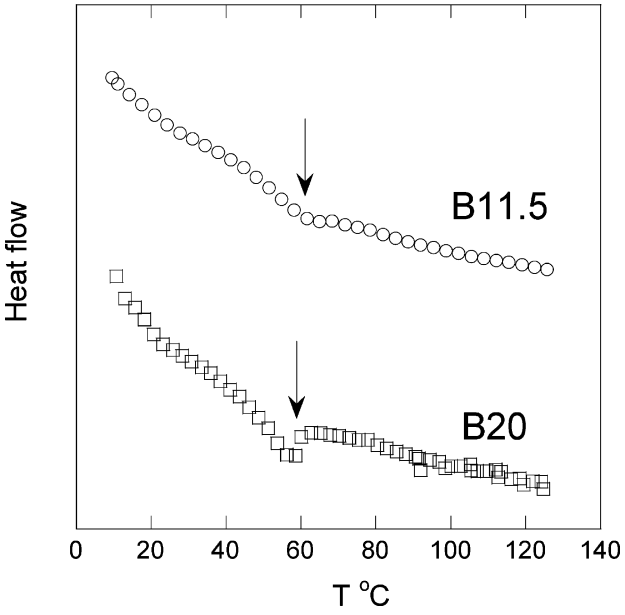

Figure 1. DSC data obtained from blends B11.5 and B20. The arrows mark the location of the change in the slope for each data set.

Differential scanning calorimetry (DSC) experiments were conducted on B11.5 and B20 with a TA 2920 instrument using a heating rate of 5 °C/min. The DSC results for both blends are shown in Figure 1. In both cases, a broad glass transition is seen. We observe a dip in the heat flow vs temperature curves in the vicinity of 60 °C (Figure 1). We take this to be the glass transition temperature (T_g) of the polystyrene-rich phase of the blends. Above T_g, the slope of the heat flow vs temperature data is nearly constant, consistent with the conclusion that our samples are liquids above T_g. We also calculated the expected value of T_g based upon the known molecular weight dependence of the T_g of polystyrene[64] [$T_g = 373 - (1.0 \times 10^5/M_v)$] and the usual mixing rule: $T_g^{-1} = \sum_i x_i/T_{g,i}$, where x_i and $T_{g,i}$ are the weight fraction and T_g of each component and M_v is the viscosity-averaged molecular weight. The results of this calculation indicate that the T_g of each blend would be less than 60 °C if the polystyrene-rich phase contained 5% polyisoprene. Because of our interest in the thermal motion of fluid structures, we restrict our attention to XPCS data obtained above 60 °C.

XPCS experiments, conducted at beamline 8-ID at the Advanced Photon Source at Argonne National Lab, yielded $g_2(q,t)$ where the magnitude of the scattering vector, $q = 4\pi \sin(\theta/2)/\lambda$, θ is the scattering angle, and λ is the wavelength of the incident beam. A more detailed explanation of the experimental setup can be found in refs 1 and 2. Two different cameras were utilized to measure $g_2(q,t)$. To access slower times, which were in the range of around 0.5−1200 s for our experiments, the scattering intensity was recorded by a direct-illuminated charge-coupled device (CCD) area detector (Princeton Instruments LCX-1300). To access faster times, which were in the range of 0.05−100 s for our experiments, the scattering intensity was recorded by a SMD 1M60 charge-coupled device (CCD) detector modified for direct illumination by X-rays.[1] In both cases, the detector was situated 3.4 m after the sample and $\lambda = 1.69$ Å.

Static small-angle X-ray scattering (SAXS) experiments were also conducted at beamline 8-ID at the Advanced Photon Source at Argonne National Lab, using the same experimental setup as the XPCS experiments. In this case the static scattering profile, $I(q)$, is measured as a function of q. To prepare the samples for the XPCS and SAXS experiments, the freeze-dried blends were placed in a sample holder containing two 1.5 mm diameter holes. One hole was filled with the sample, and the second hole remained empty for an open beam measurement. The sample was then

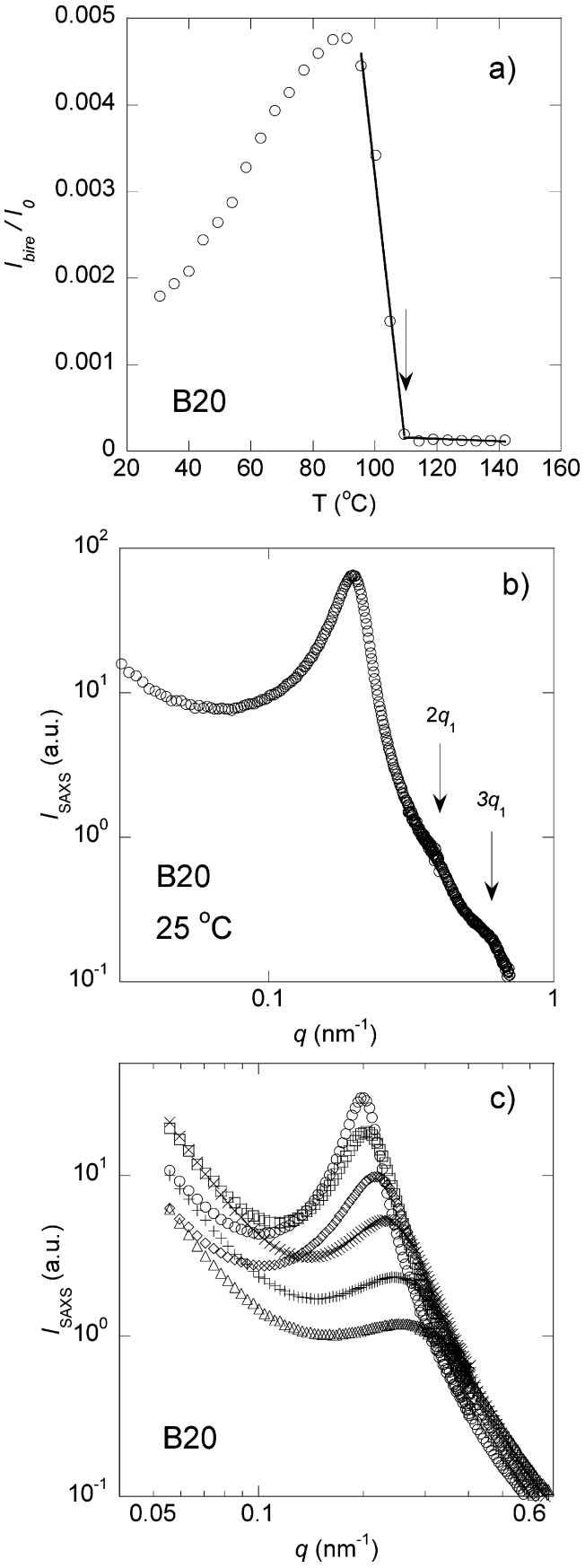

Figure 2. (a) Birefringence data obtained from blend B20 (arrow indicates the transition from a lamellar phase to a homogeneous phase). (b) SAXS data obtained from blend B20 at 25 °C in which the secondary and tertiary peaks are visible (indicated by arrows at $q_2 = 2q_1$ and $q_3 = 3q_1$). (c) SAXS data obtained from blend B20 at selected temperatures: 65 (○), 75 (□), 85 (◇), 95 (×), 105 (+), and 115 °C (△).

annealed at 110 °C to eliminate bubbles. All of the X-ray scattering profiles were azimuthally symmetric even in the temperature range where our samples had a lamellar morphology. In many cases, scattering from ordered systems (e.g., an ordered block copolymer melt) contain static speckles due to the presence of large grains at a fixed orientation in the scattering volume. The absence of such features in our samples indicates that the grains are very small and/or they are not static on the time scale of our experiments.

Birefringence experiments were conducted utilizing an experimental setup described previously.[65] To prepare the samples for birefringence experiments, the freeze-dried blends were placed on top of a quartz disk with a 1 mm aluminum spacer and annealed at 110 °C to remove any bubbles. A second quartz disk was then placed on top of the polymer. The sample was pressed together and annealed for 10 min at 110 °C to erase the thermal history.

Characterization of Equilibrium Phase Behavior

Before discussing the dynamical properties of the multicomponent blends, it is important to characterize the equilibrium phase behavior of the blends (B11.5 and B20, see Table 2). On the basis of previous studies of A/B/A−B blends,[13−17] we expect blend B20 to be lamellar. The temperature dependence of the birefringence signal (I_{bire}), normalized by the intensity of the laser beam with uncrossed polarizers (I_0), obtained from blend B20 is shown in Figure 2a. A sharp decrease in the signal is observed at $T = 110$ °C. This is a standard signature of the disordering of a lamellar phase. We thus conclude that a transition from a lamellar phase to a homogeneous phase occurs in B20 at 110 ± 3 °C.

SAXS experiments enable more complete characterization of blend B20. The scattering intensity, I, as a function of scattering vector, q, obtained from this blend at 25 °C is shown in Figure 2b. The increase in the measured $I(q)$ at $q < 0.05$ nm^{-1} is attributed to beam leakage near the beam stop and is ignored in this paper. A primary peak is observed at $q_{peak} = 0.20$ nm^{-1}. The sharpness of the peak indicates the presence of an ordered phase. In addition, we see weak signatures of higher order scattering peaks corresponding to a lamellar phase; additional peaks are located at $q_2 = 2q_1$ and $q_3 = 3q_1$ where q_1 is the location of the primary peak seen in Figure 2b. Our ability to observe higher order scattering peaks was dependent on thermal history. We conducted experiments on several independent B20 samples. We were only able to observe higher order peaks in one of them. We attribute this to the lack of strict control over the drying and annealing step in the vacuum oven at 110 °C. However, the characteristics of the primary peak were readily reproducible. The temperature dependence of the primary SAXS peak of blend B20 is shown in Figure 2c. The peak intensity decreases and the peak width increases with increasing temperature. There are, however, no qualitative changes in the SAXS profiles at the order−disorder transition. Similar effects are observed in weakly ordered diblock copolymer melts.[66]

On the basis of previous studies of A/B/A−B blends, we expected sample B11.5 to form a microemulsion.[13−17] The SAXS profiles for blend B11.5 are shown in Figure 3. In contrast to Figure 2b, there is now a broad primary peak, characteristic of a microemulsion. We use the well-established Teubner−Strey (T−S) equation[67] to analyze the scattering profiles. (The scattering profiles obtained from B20 were not consistent with the T−S equation.) The T−S equation for the scattering intensity is

$$I(q) = \frac{1}{a + bq^2 + cq^4} \tag{4}$$

where a, b, and c are fitting parameters. The fitting constants

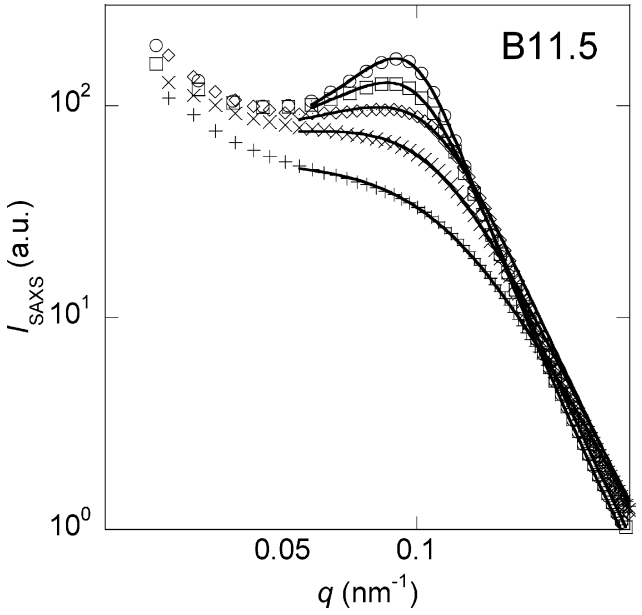

Figure 3. SAXS data obtained from blend B11.5 at selected temperatures: 65 (○), 75 (□), 85 (◇), 95 (×), and 105 °C (+). The solid lines are the Teubner−Strey scattering profile fit to the data (eq 4).

Table 3. Teubner−Strey Fitting Parameters for Blend B11.5

T (°C)	a (cm)	b (cm nm^2)	c (cm nm^4)	d (nm)	ξ (nm)	f_a
65	0.0163	−2.61	166.5	66.7	31.3	−0.793
70	0.0155	−2.34	154.4	67.0	28.6	−0.755
75	0.0147	−1.96	139.2	67.5	24.9	−0.686
80	0.0159	−1.85	121.0	64.3	22.9	−0.667
85	0.0139	−0.518	18.3	43.5	12.2	−0.514
90	0.0140	−0.378	17.0	44.6	10.7	−0.388
95	0.0141	−0.217	16.1	46.6	9.3	−0.227
100	0.0147	−0.000160	15.0	50.2	8.0	−0.00017
105	0.0187	0.215	14.2	52.5	6.8	0.209
110	0.0317	0.462	12.7	49.8	5.4	0.364

enable determination of the domain spacing, d, correlation length, ξ, and amphiphilicity factor, f_a, given by

$$\xi = \left[\frac{1}{2}\left(\frac{a}{c}\right)^{1/2} + \frac{1}{4}\frac{b}{c}\right]^{-1/2} \quad (5)$$

$$d = 2\pi\left[\frac{1}{2}\left(\frac{a}{c}\right)^{1/2} - \frac{1}{4}\frac{b}{c}\right]^{-1/2} \quad (6)$$

$$f_a = \frac{b}{2\sqrt{ac}} \quad (7)$$

All of the T−S parameters obtained from blend B11.5 are reported in Table 3. The amphiphilicity factor $f_a \rightarrow 0$ at $T = 103 \pm 3$ °C. In oil/water/surfactant systems, this indicates a transition from a weakly structured microemulsion to a strongly structured microemulsion.[68] In polymeric systems, previous authors have concluded this Lifshitz line ($f_a \rightarrow 0$) is not an indicator of a structural transition.[44]

We did not conduct birefringence experiments on B11.5 because it was cloudy. This is not unexpected due to the large size of the microemulsion structure ($d = 67$ nm at 65 °C). One previous study which utilized a bicontinuous microemulsion with $d \cong 75$ nm reported observing a blue tint to the sample due to light scattering from the microstructure.[14,56] Furthermore, in another study in which the size of the microemulsion was much larger ($d \cong 500$ nm), the sample was turbid.[69] Thus, because of the low diblock copolymer content in polymer bicontinuous microemulsions and formation of large structures, it is not unreasonable to obtain samples that are not optically clear.

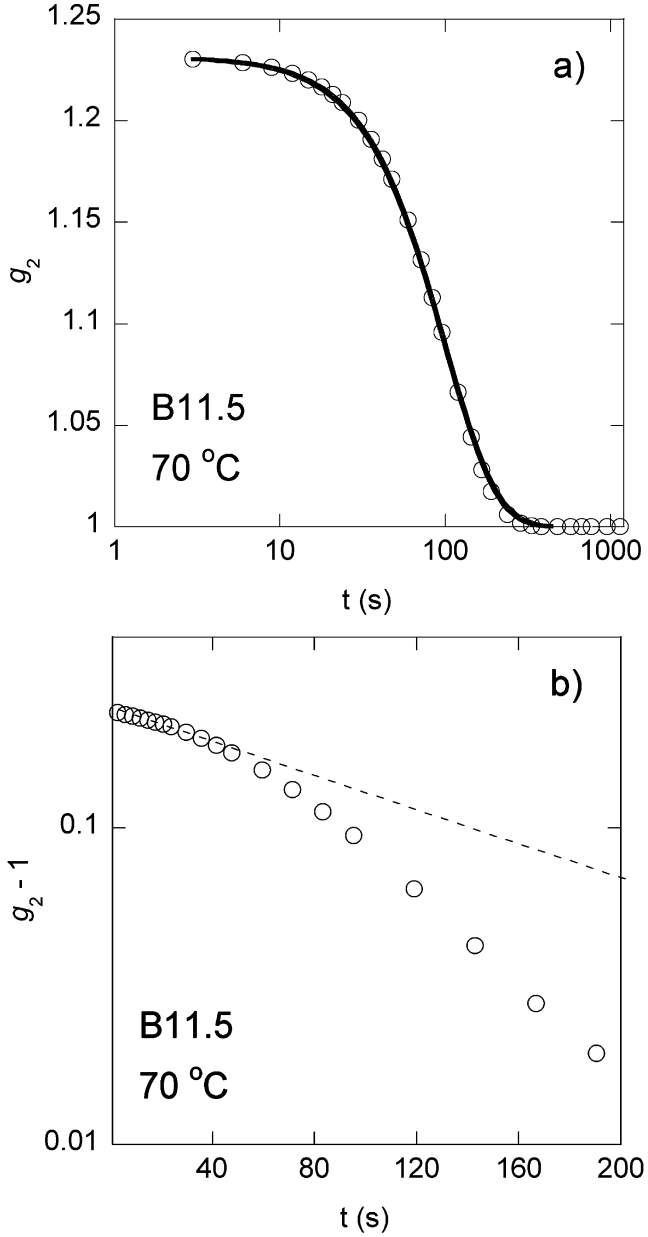

Figure 4. (a) g_2 vs t for blend B11.5 at 70 °C. The solid line is a fit of eq 3 to the data. (b) ($g_2 - 1$) vs t on a semilog plot for blend B11.5 at 70 °C. The dotted line represents an exponential curve in which $\alpha = 1$. In contrast, the data set curves downward.

Characterization of Dynamical Behavior of Microemulsions and Lamellae

XPCS experiments on blend B11.5 enabled the determination of g_2 as a function of both q and t at temperatures between 65 and 95 °C. Above 95 °C, the decay of g_2 was too rapid and beyond the fast time limit of our instrument (i.e., a constant value of unity was measured at all accessible t values). The low-temperature limit is above the measured T_g of the blends. All of the data were obtained after annealing the sample at 110 °C to erase the effect of thermal and mechanical history. Figure 4a shows the 70 °C results for g_2 at $q = q_{peak}$, where q_{peak} is the location of the structure factor primary peak maximum (the results were obtained using the Princeton Instruments camera). The function decays to 1 well within the accessible time range.

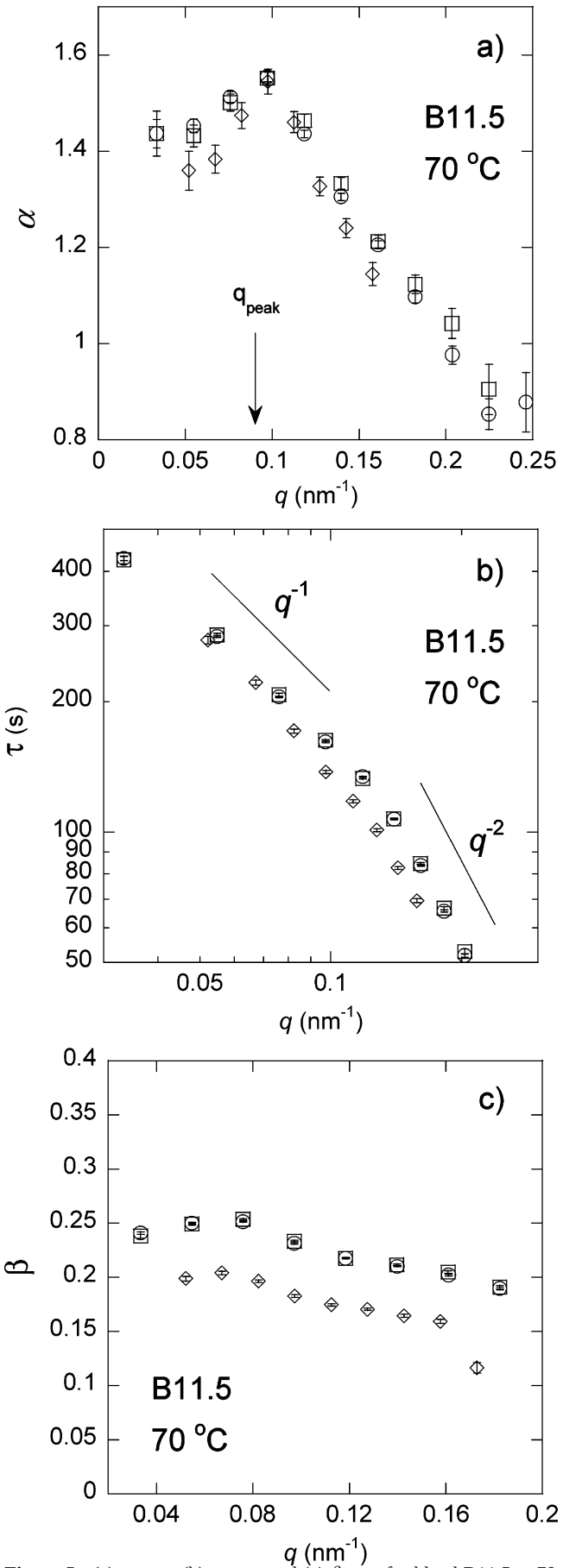

Figure 5. (a) α vs q, (b) τ vs q, and (c) β vs q for blend B11.5 at 70 °C. Two independent measurements were made on the same sample (○, □), and a third measurement was made on a separate sample (◇). In (a) the arrow indicates the q value of the structure factor peak.

It is instructive to examine these data on a semilog plot of $(g_2 - 1)$ vs t, as shown in Figure 4b. An exponential decay would be a straight line on this plot. However, as observed in Figure 4b, the function $(g_2 - 1)$ curves downward, indicating that the decay of the correlation function is more rapid than an exponential function. We use eq 3 to fit the time dependence of g_2, and the resulting least-squares fit with τ, α, and β as adjustable parameters is indicated by the curve in Figure 4a. It is clear that α is significantly greater than unity, as qualitatively anticipated from the data shown in Figure 4b (the semilog plot). The value of α determined at $q = q_{peak}$ and 70 °C is 1.55. The experimental uncertainty in our determination of α is less than 5%. We have thus ruled out both exponential and stretched exponential behavior at 70 °C.

To establish the repeatability of the XPCS experiments, we prepared two separate B11.5 samples and ran one of the samples twice (in each case the Princeton Instruments camera was used). In Figure 5 we show the q dependence of τ, α, and β at 70 °C for all three independent measurements. The experimental scatter from the three independent runs is comparable to experimental uncertainty (size of the error bars in Figure 5). At 70 °C, B11.5 exhibits a condensed exponential correlation function [$\alpha(q) > 1$] at most accessible q values. $\alpha(q)$ peaks at a value of about $\alpha = 1.55$ at $q = 0.10$ nm^{-1} (this is near the structure factor peak located at $q_{peak} = 0.09$ nm^{-1}) and decays rapidly with increasing q to a value of $\alpha = 0.9$ at $q = 0.25$ nm^{-1}. In Figure 5b, τ obtained from B11.5 at 70 °C is reported as a function of q. In the $q < q_{peak}$ (of the structure factor) regime, $\tau \sim q^{-1}$, while at $q > q_{peak}$ $\tau \sim q^{-2}$ (see solid lines in Figure 5b). The crossover between the two regimes is broad. Normally diffusive motion on long length scales leads to exponential relaxation functions and $\tau \sim q^{-2}$. To the contrary, we obtain $\tau \sim q^{-2}$ behavior on short length scales ($q > q_{peak}$). Sample B11.5 at 70 °C is thus characterized by at least three different dynamical behaviors: $\tau \sim q^{-2}$ when $q > q_{peak}$, $\tau \sim q^{-1}$ when $q < q_{peak}$, and the expected $\tau \sim q^{-2}$ when $q \ll q_{peak}$. (The behavior at $q \ll q_{peak}$ was not accessed in our XPCS experiments; however, such behavior has been reported on the basis of LPCS experiments on similar A/B/A−B blends in ref 44.) For completeness, we present the β obtained from B11.5 at 70 °C as a function of q in Figure 5c. This parameter, which is related to instrumental parameters (scattering volume, beam coherence, detector efficiency, etc.) lies between 0.15 and 0.25, regardless of temperature and sample identity. We have no explanation for the observed variation in β.

All of the g_2 functions determined from our blends were consistent with eq 3. Nonlinear fits similar to those shown in Figure 4a were used to determine the dependence of τ and α on q and T. Figure 6 summarizes these results for blend B11.5. (The data at 65−70 °C were obtained with the Princeton Instruments camera, and those at $T \geq 75$ °C were obtained with the SMD camera.) As the temperature is increased from 65 to 85 °C, $\alpha(q)$ decreases in magnitude at all values of q. At 85, 90, and 95 °C, α lies in the 0.6−0.8 range and is independent of temperature. Similar values of α (near $\alpha = 2/3$) have been observed previously in polymer vesicles and small molecule microemulsions and lamellae.[3,9−12] It is also apparent that α decreases at q values away from q_{peak} of the structure factor, regardless of the temperature. It is worth noting that previous dynamic light scattering studies conducted on polymer microemulsions probed length scales much larger than the domain size of the microemulsion structure. In that case, single exponentials, i.e., $\alpha = 1$, were used to fit the data.[17,44] It appears that condensed exponential behavior, i.e., $\alpha > 1$, occurs on

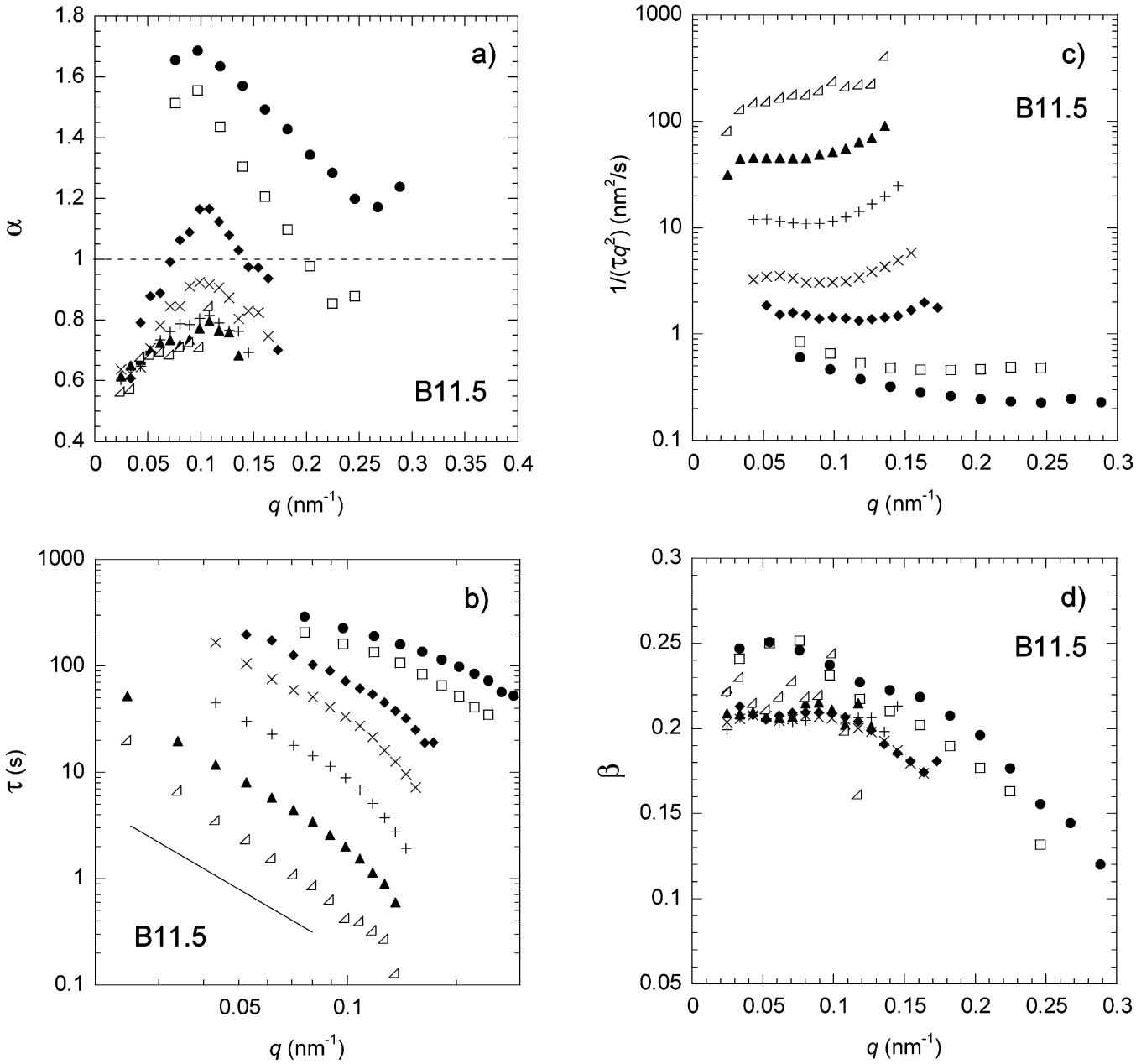

Figure 6. (a) α vs q, (b) τ vs q, (c) $1/(\tau q^2)$ vs q, and (d) β vs q for blend B11.5 at $T = 65$ (●), 70 (□), 75 (◆), 80 (×), 85 (+), 90 (▲), and 95 °C (right pointing △).

length scales comparable to the domain size. The relaxation time $\tau(q)$ was found to decrease rapidly as the temperature is increased, as shown in Figure 6b. Hennes and Gompper predicted the occurrence of a peak in τ vs q at $q = q_{peak}$ of the structure factor for a microemulsion or sponge phase in which $\xi/d = 8.9$.[70] When $\xi/d < 3.5$, τ was predicted to be a monotonic function of q.[70] In blend B11.5, $\xi/d < 1$. Perhaps a peak would be observed in $\tau(q)$ of B11.5 if ξ were larger. It is important to note that the theory does not account for condensed exponential correlation functions.

It is instructive to plot $1/\tau q^2$ vs q, as we have done in Figure 6c. The q-independent plateaus seen in Figure 6c suggest that the relaxation process observed by XPCS may have a diffusive character. We cannot be certain about the implication of the plateaus because diffusive processes are characterized by exponential correlation functions. A slight upturn in the data is observed on the low-q portion of the plot at low temperatures, and another upturn is observed on the high-q portion of the plot at high temperatures. It is possible that there is a very broad peak in $1/\tau q^2$ vs q at all temperatures in B11.5 and that due to our limited range of accessible times we are missing parts of the broad peak. The existence of a peak would be in agreement with the predictions of Hennes and Gompper,[70] and perhaps the low value of ξ/d for this microemulsion is the reason that the peak is very broad. For completeness, we present the β obtained from B11.5 as a function of q in Figure 6d.

The procedure described above was used to analyze XPCS data obtained from blend B20 between 65 and 80 °C (all data were obtained with the SMD camera). Most samples of blend B20 were annealed at 110 °C before collecting XPCS data. One B20 sample was annealed at 140 °C before collecting XPCS data, and no effect was observed on the dynamic results. Above 80 °C, the decay of g_2 was too rapid and beyond the fast time limit of our instrument. In the case of B20, most of the data sets were consistent with eq 3. However, some of the data sets obtained in the ordered state contained a slow mode. The characteristics of this mode are discussed in the Appendix and are not included in the discussion that follows here. Figure 7a

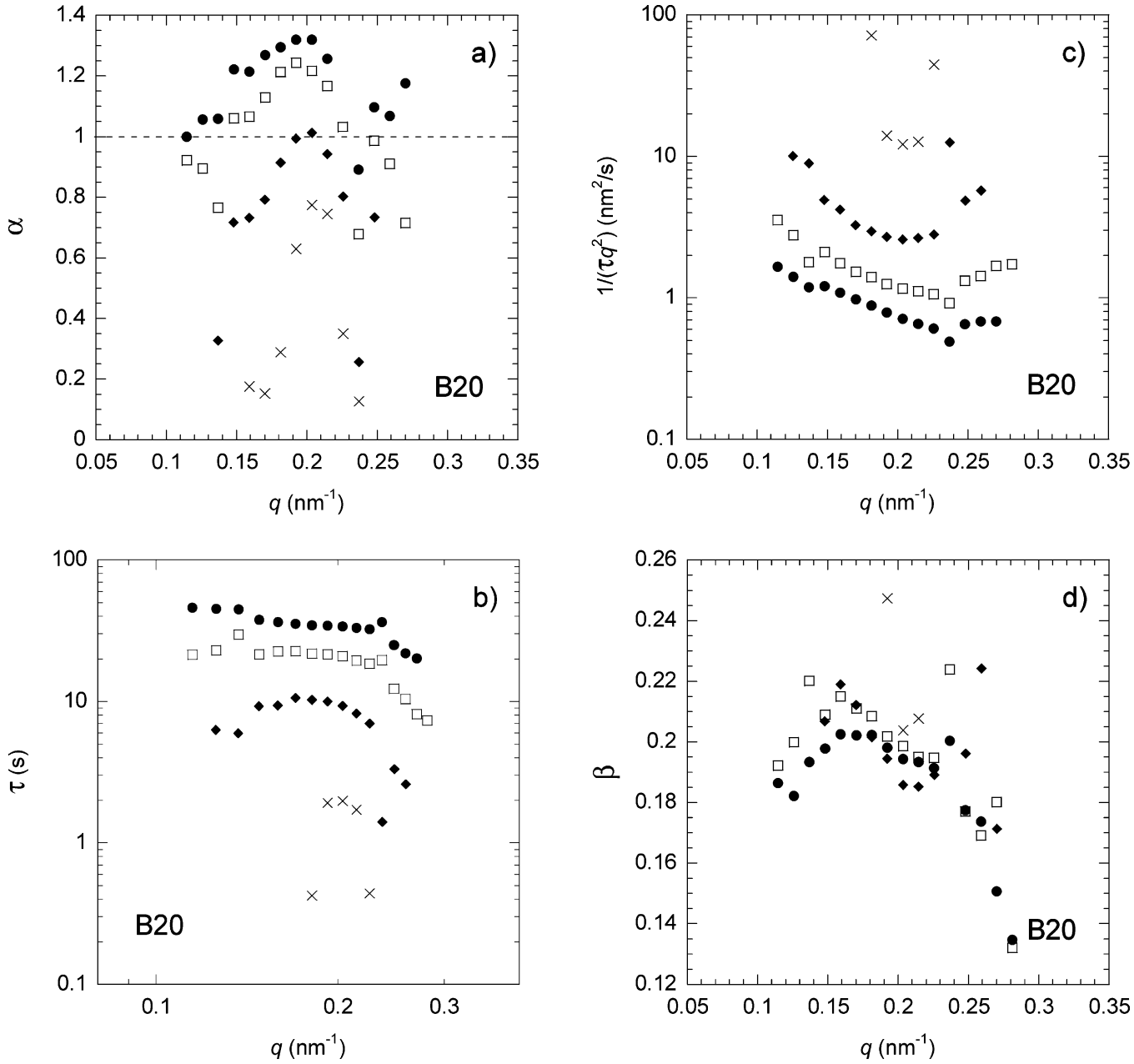

Figure 7. (a) α vs q, (b) τ vs q, (c) $1/(\tau q^2)$ vs q, and (d) β vs q for blend B20 at $T = 65$ (●), 70 (□), 75 (◆), and 80 °C (×).

shows the q dependence of α. As was the case with the B11.5 sample, we obtain a peak in α at $q = q_{peak}$. We observe condensed exponential correlation functions at 65 and 70 °C ($\alpha > 1$) and stretched exponential correlation functions at 75 and 80 °C. It is evident that both the microemulsion and lamellar phases show condensed exponential behavior at low temperatures. In Figure 7b we plot τ as a function of q. It is evident that τ decreases rapidly with increasing temperature. The A−B diblock copolymer is the longest chain in our A/B/A−B mixtures. If the viscosity of the mixture were an important factor in the relaxation processes that we have measured by XPCS, then B20 would have slower relaxation than B11.5. Comparing Figures 6b and 7b, it is obvious that XPCS-determined τ values obtained from B20 at a given temperature are significantly smaller than that obtained from B11.5. At $q = q_{peak}$, for example, τ of B20 is about a factor of 10 smaller than that in B11.5. It is interesting that in blend B20 τ is almost independent of q at $T = 65$ °C (Figure 7b). The width of the q-independent plateau decreases with increasing temperature. Pan et al. have observed q-independent relaxation in LPCS measurements on block copolymers[63] which was ascribed to the relative motion of the centers of mass of the two blocks on a single chain. We cannot make such claims in our systems mainly due to the fact that our correlation functions are nonexponential. It is conceivable, however, that similar local motion is being probed in our XPCS measurements in B20. As the temperature is increased, the τ vs q data in Figure 7b exhibit maxima in the vicinity of $q = q_{peak}$. This kind of behavior is anticipated in disordered fluctuating phases near a critical point and is sometimes called de Gennes narrowing.[71] Such a peak in $\tau(q)$ has been observed in a wide variety of systems including polymer systems.[72−77] In Figure 7c we plot $1/\tau q^2$ as a function of q at different temperatures for B20. We observe a minimum in this plot as anticipated from systems exhibiting de Gennes narrowing. For completeness, we present the β obtained from B20 as a function of q in Figure 7d.

In Figure 8 we show the temperature dependence of the apparent diffusion coefficient, $D = 1/\tau q^2$, of B20 (squares). The value of τ used to calculate D for blend B20 was obtained from the minima in the data in Figure 7c. We also plot the temperature

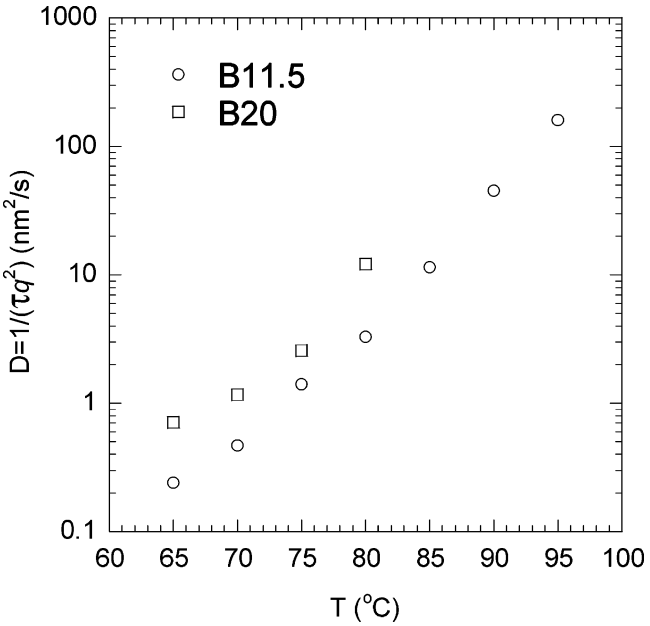

Figure 8. Diffusion coefficient, $D = 1/(\tau q^2)$, obtained from the plateau in Figure 6c for blend B11.5 (circles) and obtained from the peak location in Figure 7c for blend B20 (squares).

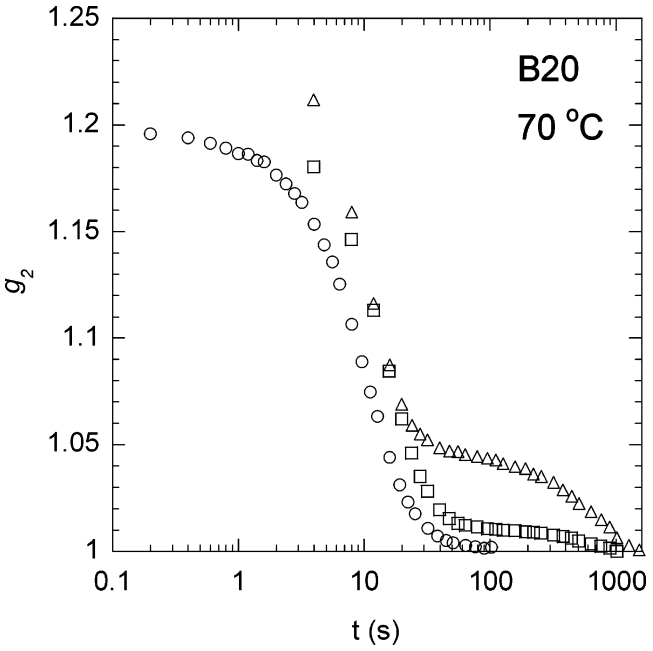

Figure 9. g_2 vs t for blend B20 at 70 °C. Three independent experiments were conducted. Data were obtained with the first sample utilizing the SMD camera (○) and Princeton Instruments camera (□), and data were obtained on a second sample utilizing the Princeton Instruments camera (△).

dependence of the apparent diffusion coefficient, $D = 1/\tau q^2$, of blend B11.5 (circles). The value of τ used to calculate D for blend B11.5 was extracted from the plateaus in Figure 6c. The temperature dependencies of D obtained from B11.5 and B20 are similar (Figure 8).

The most surprising result is our observation of condensed exponential correlation functions as documented in Figures 4b, 6a, and 7a. We do not have a good explanation for this observation. It is, perhaps, worth noting that XPCS measurements on a polystyrene-*b*-polyisoprene diblock copolymer yielded exponential correlation functions.[78] This suggests that the condensed exponential correlation functions in PS/PI/PS−PI mixtures do not arise from artifacts such as radiation damage or radiation-induced temperature gradients. If we interpret the slope of the $\log(g_2 - 1)$ vs t curve, e.g., Figure 4b, as an indication of relaxation time, then it appears as though structural relaxation speeds up with increasing time. Since we must be probing larger length scales as time increases, we conclude that relaxation across large length scales is more rapid that that on small length scales. A possible reason for this is the spontaneous breakup (and uncorrelated reassembly) of microstructure. We thus propose that on small time and length scales, where the $\log(g_2 - 1)$ vs t curve is approximately linear, we observe classical microstructural relaxation. For B11.5 at 70 °C, for example, the data in Figure 4b suggest that a single exponential is a good approximation for $t < 20$ s. We thus propose that microstructure breaks up on time scales comparable to 20 s and results in a rapid decay of the correlation function. We recognize that similar processes occur in other systems such as wormlike micelles[79−81] and that there are no reports of condensed exponential correlation functions in these systems. This suggests that the processes that result in structural breakup in samples B11.5 and B20 are significantly different from those occurring in classical systems such as wormlike micelles.

Conclusion

XPCS experiments were conducted on two multicomponent PS/PI/PS−PI blends: B11.5 (a microemulsion phase) and B20 (a lamellar phase). Previous studies on membrane-containing systems, such as small molecule microemulsions and polymer vesicles, revealed stretched exponential correlation functions, $g_2(q,t) \sim \exp\{-[t/\tau(q)]^\alpha\}$, with stretching exponent, $\alpha \sim 2/3$. In contrast, the correlation functions of B11.5 and B20 were found to decay faster than an exponential curve, i.e., $\alpha > 1$. We use the term condensed exponential to describe these functions. In our systems, α was as large as 1.7. We suggest that this unusual behavior is due to the spontaneous breakup of the self-assembled structures. Condensed exponential correlation functions have been observed in colloidal gels far from equilibrium.[82] Our observation of similar behavior in a non-stressed polymeric system, however, could not be predicted. Further work is needed to clarify the underpinnings of the dynamical data presented here.

Acknowledgment. This material is based upon work supported by the National Science Foundation under Grants 0305711 and 0504122. The APS is supported by the U.S. DOE under Contract No. W-31-109-Eng-38. A.J.P. gratefully acknowledges additional support from Tyco Electronics.

Appendix. Observation of a Slow Mode in Blend B20

To verify the robustness of the results reported for blend B20, multiple samples were investigated. Two separate samples were utilized, and two different cameras were also used to obtain data in varying time ranges. The data that have been presented in the main body of this paper were obtained with one of the samples utilizing the SMD camera. However, data were obtained on the same sample utilizing the Princeton Instruments camera, and data were obtained on a second sample, also with the Princeton Instruments camera. The results from all three experiments at 70 °C are shown in Figure 9 (all data are shown for $q = q_{peak}$).

The data obtained from the SMD camera (circles in Figure 9) were the basis for all of the results reported in this paper at 70 °C for blend B20. In this case, the correlation function clearly decays to 1 before 100 s. When the same sample was analyzed

with the Princeton Instruments camera (squares in Figure 9), an initial decay is observed which is consistent with the relaxation time observed from the SMD camera. In contrast to the data obtained from the SMD camera, however, the correlation function plateaus at a value greater than 1, and then there is a second, longer time decay until the correlation function finally reaches 1 by 1000 s. It is not clear why the SMD camera did not show evidence of this longer time decay. It would be expected that the data obtained from the SMD camera would plateau at a value of the correlation function that is not equal to 1, even though the time range would not capture the longer time decay. It is possible that the SMD camera is not as sensitive as the Princeton Instruments camera and could not pick up the subtle longer time decay. An additional possibility is that there could be an effect of the thermal history of the sample, as each experiment had a slightly different thermal history. Perhaps there are grains present in the ordered B20 sample that are not reproduced to be exactly the same each time, and that is the source of the longer time decay. We repeated this experiment with a second sample and utilized the Princeton Instruments camera (triangles in Figure 9). Again, the initial decay is in agreement with the first two experiments (compare all three data sets in Figure 9), and there is also a second decay at longer times, with a location that is in agreement with the previous Princeton Instruments camera experiments (compare squares and triangles in Figure 9). This behavior was observed not only at 70 °C for blend B20, but throughout the range of measurable correlation functions (65−80 °C).

It is interesting to contrast the data obtained from blend B20 to the data obtained from blend B11.5. Even with the Princeton Instruments camera, blend B11.5 never exhibited a second decay at longer times. The data shown in Figure 4a for blend B11.5 at 70 °C clearly decay to 1. This result was observed at all temperatures, and the result was the same every time the experiment was repeated (data were obtained on blend B11.5 in three independent experiments on two separate samples). However, this is to be expected as blend B11.5 is a disordered microemulsion and does not exhibit any long-range order. Thus, the ability to attain equilibrium in B11.5 is unaffected by the annealing history (and without long-range order there will be no grain formation).

References and Notes

(1) Falus, P.; Borthwick, M. A.; Mochrie, S. G. J. *Rev. Sci. Instrum.* **2004**, *75*, 4383−4400.
(2) Sandy, A. R.; Lurio, L. B.; Mochrie, S. G. J.; Malik, A.; Stephenson, G. B.; Pelletier, J. F.; Sutton, M. *J. Synchrotron Radiat.* **1999**, *6*, 1174−1184.
(3) Falus, P.; Borthwick, M. A.; Mochrie, S. G. J. *Phys. Rev. Lett.* **2005**, *94*, Article No. 016105.
(4) Vanmegen, W.; Pusey, P. N. *Phys. Rev. A* **1991**, *43*, 5429−5441.
(5) Debenedetti, P. G. *AIChE J.* **2005**, *51*, 2391−2395.
(6) Urakawa, O.; Swallen, S. F.; Ediger, M. D.; von Meerwall, E. D. *Macromolecules* **2004**, *37*, 1558−1564.
(7) Zilman, A. G.; Granek, R. *Chem. Phys.* **2002**, *284*, 195−204.
(8) Zilman, A. G.; Granek, R. *Phys. Rev. Lett.* **1996**, *77*, 4788−4791.
(9) Monkenbusch, M.; Holderer, O.; Frielinghaus, H.; Byelov, D.; Allgaier, J.; Richter, D. *J. Phys.: Condens. Matter* **2005**, *17*, S2903−S2909.
(10) Kimura, Y.; Oizumi, J.; Hayakawa, R. *Mol. Cryst. Liq. Cryst. Sci. Technol., Sect. A* **1999**, *332*, 3069−3077.
(11) Takeda, T.; Kawabata, Y.; Seto, H.; Komura, S.; Ghosh, S. K.; Nagao, M.; Okuhara, D. *J. Phys. Chem. Solids* **1999**, *60*, 1375−1377.
(12) Freyssingeas, E.; Roux, D. *J. Phys. II* **1997**, *7*, 913−929.
(13) Bates, F. S.; Maurer, W.; Lodge, T. P.; Schulz, M. F.; Matsen, M. W.; Almdal, K.; Mortensen, K. *Phys. Rev. Lett.* **1995**, *75*, 4429−4432.
(14) Hillmyer, M. A.; Maurer, W. W.; Lodge, T. P.; Bates, F. S.; Almdal, K. *J. Phys. Chem. B* **1999**, *103*, 4814−4824.
(15) Bates, F. S.; Maurer, W. W.; Lipic, P. M.; Hillmyer, M. A.; Almdal, K.; Mortensen, K.; Fredrickson, G. H.; Lodge, T. P. *Phys. Rev. Lett.* **1997**, *79*, 849−852.
(16) Washburn, N. R.; Lodge, T. P.; Bates, F. S. *J. Phys. Chem. B* **2000**, *104*, 6987−6997.
(17) Morkved, T. L.; Chapman, B. R.; Bates, F. S.; Lodge, T. P.; Stepanek, P.; Almdal, K. *Faraday Discuss.* **1999**, 335−350.
(18) Cohen, R. E.; Ramos, A. R. *Macromolecules* **1979**, *12*, 131−134.
(19) Datta, S.; Lohse, D. J. *Polymeric Compatibilizers*; Hanser: Cincinnati, OH, 1996.
(20) Hudson, S. D.; Jamieson, A. M. In *Polymer Blends*; Paul, C. B., Ed.; Wiley: New York, 2000; Vol. 1.
(21) Jeon, H. S.; Lee, J. H.; Balsara, N. P. *Phys. Rev. Lett.* **1997**, *79*, 3274−3277.
(22) Jeon, H. S.; Lee, J. H.; Balsara, N. P. *Macromolecules* **1998**, *31*, 3328−3339.
(23) Jeon, H. S.; Lee, J. H.; Balsara, N. P.; Newstein, M. C. *Macromolecules* **1998**, *31*, 3340−3352.
(24) Lyu, S.; Jones, T. D.; Bates, F. S.; Macosko, C. W. *Macromolecules* **2002**, *35*, 7845−7855.
(25) Tan, N. C. B.; Tai, S. K.; Briber, R. M. *Polymer* **1996**, *37*, 3509−3519.
(26) Jackson, C. L.; Sung, L.; Han, C. C. *Polym. Eng. Sci.* **1997**, *37*, 1449−1458.
(27) Sung, L.; Hess, D. B.; Jackson, C. L.; Han, C. C. *J. Polym. Res. (Taiwan)* **1996**, *3*, 139.
(28) Koizumi, S.; Hasegawa, H.; Hashimoto, T. *Macromolecules* **1994**, *27*, 7893−7906.
(29) Kielhorn, L.; Muthukumar, M. *J. Chem. Phys.* **1997**, *107*, 5588−5608.
(30) Balsara, N. P.; Jonnalagadda, S. V.; Lin, C. C.; Han, C. C.; Krishnamoorti, R. *J. Chem. Phys.* **1993**, *99*, 10011−10020.
(31) Leibler, L. *Makromol. Chem., Macromol. Symp.* **1988**, *16*, 1−17.
(32) Leibler, L. *Physica A* **1991**, *172*, 258−268.
(33) Broseta, D.; Fredrickson, G. H. *J. Chem. Phys.* **1990**, *93*, 2927−2938.
(34) Mathur, D.; Hariharan, R.; Neuman, E. B. *Polymer* **1999**, *40*, 6077−6087.
(35) Wang, Z. G.; Safran, S. A. *J. Phys. (Paris)* **1990**, *51*, 185−200.
(36) Janert, P. K.; Schick, M. *Macromolecules* **1997**, *30*, 3916−3920.
(37) Janert, P. K.; Schick, M. *Macromolecules* **1997**, *30*, 137−144.
(38) Muller, M.; Schick, M. *J. Chem. Phys.* **1996**, *105*, 8885−8901.
(39) Maric, M.; Macosko, C. W. *J. Polym. Sci., Part B: Polym. Phys.* **2002**, *40*, 346−357.
(40) Schnell, R.; Stamm, M.; Rauch, F. *Macromol. Chem. Phys.* **1999**, *200*, 1806−1812.
(41) Zhao, H. Y.; Huang, B. T. *J. Polym. Sci., Part B: Polym. Phys.* **1998**, *36*, 85−93.
(42) Ruzette, A. V.; Leibler, L. *Nat. Mater.* **2005**, *4*, 19−31.
(43) Tanaka, H.; Hasegawa, H.; Hashimoto, T. *Macromolecules* **1991**, *24*, 240−251.
(44) Morkved, T. L.; Stepanek, P.; Krishnan, K.; Bates, F. S.; Lodge, T. P. *J. Chem. Phys.* **2001**, *114*, 7247−7259.
(45) Stepanek, P.; Nallet, F.; Almdal, K. *Macromolecules* **2001**, *34*, 1090−1095.
(46) Oizumi, J.; Kimura, Y.; Ito, K.; Hayakawa, R. *Mol. Cryst. Liq. Cryst. Sci. Technol., Sect. A* **1997**, *303*, 63−71.
(47) Papadakis, C. M.; Brown, W.; Johnsen, R. M.; Posselt, D.; Almdal, K. *J. Chem. Phys.* **1996**, *104*, 1611−1625.
(48) Papadakis, C. M.; Rittig, F.; Almdal, K.; Mortensen, K.; Stepanek, P. *Eur. Phys. J. E* **2004**, *15*, 359−370.
(49) Stepanek, P.; Morkved, T. L.; Krishnan, K.; Lodge, T. P.; Bates, F. S. *Phys. A* **2002**, *314*, 411−418.
(50) Yoshida, E.; Wells, S. L.; DeSimone, J. M. *Kobunshi Ronbunshu* **2001**, *58*, 507−513.
(51) Papadakis, C. M.; Almdal, K.; Mortensen, K.; Rittig, F.; Stepanek, P. *Macromol. Symp.* **2000**, *162*, 275−290.
(52) Papadakis, C. M.; Almdal, K.; Mortensen, K.; Rittig, F.; Fleischer, G.; Stepanek, P. *Eur. Phys. J. E* **2000**, *1*, 275−283.
(53) Stepanek, P.; Morkved, T. L.; Bates, F. S.; Lodge, T. P.; Almdal, K. *Macromol. Symp.* **2000**, *149*, 107−112.
(54) Mortensen, K.; Brown, W.; Almdal, K.; Alami, E.; Jada, A. *Langmuir* **1997**, *13*, 3635−3645.
(55) Krishnan, K.; Burghardt, W. R.; Lodge, T. P.; Bates, F. S. *Langmuir* **2002**, *18*, 9676−9686.
(56) Krishnan, K.; Chapman, B.; Bates, F. S.; Lodge, T. P.; Almdal, K.; Burghardt, W. R. *J. Rheol.* **2002**, *46*, 529−554.
(57) Burghardt, W. R.; Krishnan, K.; Bates, F. S.; Lodge, T. P. *Macromolecules* **2002**, *35*, 4210−4215.
(58) Rittig, F.; Karger, J.; Papadakis, C. M.; Fleischer, G.; Almdal, K.; Stepanek, P. *Macromolecules* **2001**, *34*, 868−873.
(59) Anastasiadis, S. H. *Curr. Opin. Colloid Interface Sci.* **2000**, *5*, 324−333.
(60) Rittig, F.; Fleischer, G.; Karger, J.; Papadakis, C. M.; Almdal, K.; Stepanek, P. *Macromolecules* **1999**, *32*, 5872−5877.

(61) Fleischer, G.; Rittig, F.; Karger, J.; Papadakis, C. M.; Mortensen, K.; Almdal, K.; Stepanek, P. *J. Chem. Phys.* **1999**, *111*, 2789−2796.
(62) Hamersky, M. W.; Hillmyer, M. A.; Tirrell, M.; Bates, F. S.; Lodge, T. P.; von Meerwall, E. D. *Macromolecules* **1998**, *31*, 5363−5370.
(63) Pan, C.; Maurer, W.; Liu, Z.; Lodge, T. P.; Stepanek, P.; Vonmeerwall, E. D.; Watanabe, H. *Macromolecules* **1995**, *28*, 1643−1653.
(64) *Polymer Handbook*, 3rd ed.; John Wiley & Sons: New York, 1989.
(65) Garetz, B. A.; Newstein, M. C.; Dai, H. J.; Jonnalagadda, S. V.; Balsara, N. P. *Macromolecules* **1993**, *26*, 3151−3155.
(66) Roe, R. J.; Fishkis, M.; Chang, J. C. *Macromolecules* **1981**, *14*, 1091−1103.
(67) Teubner, M.; Strey, R. *J. Chem. Phys.* **1987**, *87*, 3195−3200.
(68) D'Arrigo, G.; Giordano, R.; Teixeira, J. *Eur. Phys. J. E* **2003**, *10*, 135−142.
(69) Lee, J. H.; Ruegg, M. L.; Balsara, N. P.; Zhu, Y. Q.; Gido, S. P.; Krishnamoorti, R.; Kim, M. H. *Macromolecules* **2003**, *36*, 6537−6548.
(70) Hennes, M.; Gompper, G. *Phys. Rev. E* **1996**, *54*, 3811−3831.
(71) de Gennes, P. G. *Physica* **1959**, *25*, 825−839.
(72) Arbe, A. *Phys. B: Condens. Matter* **2004**, *350*, 178−185.
(73) Neelakantan, A.; Maranas, J. K. *J. Chem. Phys.* **2004**, *120*, 1617−1626.
(74) Mochrie, S. G. J. *Macromolecules* **2003**, *36*, 5013−5019.
(75) Saboungi, M. L.; Price, D. L.; Mao, G. M.; Fernandez-Perea, R.; Borodin, O.; Smith, G. D.; Armand, M.; Howells, W. S. *Solid State Ionics* **2002**, *147*, 225−236.
(76) Chang, R. W.; Yethiraj, A. *J. Chem. Phys.* **2002**, *116*, 5284−5298.
(77) Richter, D.; Arbe, A.; Colmenero, J.; Monkenbusch, M.; Farago, B.; Faust, R. *Macromolecules* **1998**, *31*, 1133−1143.
(78) Patel, A. J.; Narayanan, S.; Sandy, A. R.; Mochrie, S. G. J.; Garetz, B. A.; Watanabe, H.; Balsara, N. P. *Phys. Rev. Lett.* **2006**, *96*, Article No. 257801.
(79) Marques, C. M.; Turner, M. S.; Cates, M. E. *J. Non-Cryst. Solids* **1994**, *172*, 1168−1172.
(80) Miyahara, M.; Kawasaki, H.; Garamus, V. M.; Nemoto, N.; Kakehashi, R.; Tanaka, S.; Annaka, M.; Maeda, H. *Colloids Surf., B* **2004**, *38*, 131−138.
(81) Herzog, B.; Huber, K.; Rennie, A. R. *J. Colloid Interface Sci.* **1994**, *164*, 370−381.
(82) Cipelletti, L.; Manley, S.; Ball, R. C.; Weitz, D. A. *Phys. Rev. Lett.* **2000**, *84*, 2275−2278.

MA061183Y